Journal of Nuclear Materials 384 (2009) 315–321

Contents lists available at ScienceDirect

Journal of Nuclear Materials

journal homepage: www.elsevier.com/locate/jnucmat

Temperature accelerated dynamics study of migration process of oxygen defects in UO_2

Takashi Ichinomiya [a,*], Blas P. Uberuaga [b], Kurt E. Sickafus [b], Yasumasa Nishiura [a], Mitsuhiro Itakura [c], Ying Chen [d], Yasunori Kaneta [d], Motoyasu Kinoshita [c,d,e]

[a] Nonlinear Science and Computation, Research Institute for Electronic Science, Hokkaido University, Kita-ku Kita-12 Nishi-6, Sapporo, Hokkaido 060-0812, Japan
[b] Los Alamos National Laboratory, Los Alamos, New Mexico 87545, USA
[c] Japan Atomic Energy Agency, Ibaraki 319-1195, Japan
[d] Department of Quantum Engineering and System Science, The University of Tokyo, Hongo 7-3-1, Tokyo 113-8656, Japan
[e] Central Research Institute of Electric Power Industry, Tokyo 201-8511, Japan

ARTICLE INFO

Article history:
Received 30 June 2008
Accepted 3 December 2008

PACS:
31.15.xv
61.72.J–
61.80.–x

ABSTRACT

We studied the migration dynamics of oxygen point defects in UO_2 which is the primary ceramic fuel for light-water reactors. Temperature accelerated dynamics simulations are performed for several initial conditions. Though the migration of the single interstitial is much slower than that of the vacancy, clustered interstitial shows faster migration than those. This observation gives us important insight on the formation mechanism of high-burnup restructuring, including planar defects and grain sub-division (the rim structure), found in UO_2.

© 2008 Elsevier B.V. All rights reserved.

1. Introduction

The nuclear fuel industry has a need to increase fuel burnup in light-water reactors (LWR). When the inventory of fission products is accumulated at high-burnup, the driving force for fuel rod failure emerges, causing serious problems in reliability and safety. Therefore, large retention capability is essential for the development of new fuel materials which permit high-burnup. The retention capability of the UO_2 fuel pellets changes its performance during the burnup process. Such changes are caused by the restructuring of the material, and two restructuring stages are known to exist in the outer edge of the pellet where the temperature is between 500 and 700 °C and thermal activation is negligible. The first restructuring process is the planar fault formation around 50 MWd/kg U, and the second is the grain sub-division and coarsened bubble formation at around 70 MWd/kg U [1–4]. The latter observation is sometimes called the 'rim structure', or 'high-burnup structure'.

The mechanism of the rim structure formation is still under investigation. However, some experiments suggest the importance of planar defects. First, it is generally known that the structure first appears adjacent to free surfaces where constraints for atoms are different from that in the bulk, namely it is easier to form two-dimensional faults such as sub-grain boundaries. Second, one typical structure observed is the Cauliflower structure, which is created by grain sub-division on planar faults. Third, as mentioned above, it is observed that some planar structures appear well before the grain sub-division. A detailed investigation of the planar structure using TEM was performed [5–7], which revealed it to be a crystallographically [1 1 1] plane. In terms of LWR fuel performance, this planar structure may provide (1) a path for fission gas transport and release to the outside of the pellet, and (2) an initiation site for the rim structure formation. Therefore the study of the formation mechanism of the planar structure is important.

With regards to the irradiation-induced restructuring in fuel ceramic pellets, one important effect of fission tracks is electronic excitation around the area of the track. Simulating UO_2 by the same fluorite ionic compound CeO_2, in-situ irradiation of electron and heavy-ion was performed [8,9]. It was found that the planar structure was formed by electron irradiation. This planar structure was on [1 1 1] planes and the fault was estimated to be stabilized by the presence of neutral oxygen gas. These simulation experiments indicate that once extra oxygen is available in oxides with the fluorite structure, a large amount of oxygen agglomerates may form planar structures on [1 1 1] planes.

The driving force of oxygen migration in nuclear fuel is overlapping fission tracks. The detailed time and space structure of fission

* Corresponding author. Current address: Department of Mathematics, Kyoto University, Kyoto, Japan.
E-mail address: miya@math.kyoto-u.ac.jp (T. Ichinomiya).

0022-3115/$ - see front matter © 2008 Elsevier B.V. All rights reserved.
doi:10.1016/j.jnucmat.2008.12.040

tracks is not well understood at present and is under study. The works of Johnson and Bringa, and also Toulemonde et al. indicate that an explosive displacement of anions occurs at the core of the fission track [10,11]. The anion atoms are temporarily dispersed outside the track core and the surrounding area may have excess oxygen. Experimentally, under thermal equilibrium, excess oxygen (hyper stoichiometric state) leads to diffusive transport for both anions and cations as investigated by Matzke [12]. Therefore excess oxygen is a very important basic state for finding the mechanism of restructuring in high-burnup fuel, including the formation process of the planar structure and the rim structure.

These results indicate that the behavior of defect ordering of anions is the most essential and important behavior for the restructuring of UO_2. In this context, we investigated the behavior of anion defects, especially stressing the behavior of excess oxygen in the fluorite structure.

Though there are many theoretical studies on defects in UO_2 by both first-principle calculations [13] and molecular dynamics simulations [14], there is a difficulty in the simulation of the dynamics of anion defects. After the passing of fission track, the temperature is kept high enough to move the anions for nearly 20 ps. Some of the processes initiated during the first few pico seconds may last for time-scales of hundreds of pico seconds, which cannot be treated by first-principle calculations or molecular dynamical simulations. In order to investigate such long-time behavior, we used the temperature accelerated dynamics (TAD) method, developed by Sørensen and Voter [15]. The key idea of this method is to estimate the transition time at the low temperature of interest from the dynamics at high temperature, using the knowledge of the transition state energy. The transition state theory tells that the rate v of an activation event i with transition state energy E_i is given by the Arrhenius law,

$$v_i = v_{0,i}\exp(-E_i/k_BT), \tag{1}$$

where $v_{0,i}$ is a constant, T is temperature, and k_B is the Boltzmann constant. From this equation, we can derive the relation between t_h, the transition time at high temperature T_h, and t_l, that at low temperature T_l, as

$$t_l = t_h \exp\left(\frac{E_i}{k_BT_l} - \frac{E_i}{k_BT_h}\right). \tag{2}$$

Using this equation, we extrapolate t_l from the molecular dynamics simulation at high temperature.

2. Simulation methodology

We performed TAD simulation of defect process in UO_2. For an interatomic potential, we employed the one derived by Basak et al. [16], described by

$$f_{ij}(r) = \frac{z_iz_je^2}{r} + f_0b_{ij}\exp\left(\frac{a_{ij}-r}{b_{ij}}\right) - \frac{c_ic_j}{r^6} + f_0D_{ij}\left[\exp\{-2\beta_{ij}(r-r^*_{ij})\} - 2\exp\{-\beta_{ij}(r-r^*_{ij})\}\right], \tag{3}$$

where i, j and r represent the species of atoms and the distance between them, respectively. The parameters involved in this model are given in Table 1. Molecular dynamical simulations based on this two-body potential give good agreement with experiment and first-principle calculations [17].

Here, we need to address the problem of stoichiometry. In the Basak potential, uranium and oxygen atoms are charged, and the introduction of interstitials or vacancies breaks charge neutrality. Such non-stoichiometry causes the divergence of the energy of the system when we carry out a simulation with periodic boundary conditions. To avoid this problem, we assume that a spatially uniform charge exists to keep electroneutrality. This assumption modifies the total energy of the system, however, it does not modify the force acting on each atom.

Table 1
The values of parameters defining the Basak potential, Eq. (1) [16].

Parameters(unit)	(O,O)	(U,U)	(U,O)
z_iz_j (Å)	1.44	5.76	2.88
f_0 (kJ/mol Å)		4.07196	
a_{ij} (Å)	3.82	3.26	3.54
b_{ij} (Å)	0.327022	0.327022	0.327022
c_ic_j (kJ/mol Å^{-6})	381	0	0
D_{ij} (Å^{-1})	N.A.	N.A.	13.6765
β_{ij} (Å^{-1})	N.A.	N.A.	1.65
r^*_{ij} (Å)	N.A.	N.A.	2.369

Now we describe the details of the simulation. The size of the system is a $4\times4\times4$ superlattice, which corresponds to a $U_{256}O_{512}$ crystal. As a boundary condition, we employ periodic boundary conditions. Unfortunately, a TAD simulation with constant pressure is impossible, due to the issues in calculating the transition state energy, so we performed the simulation with NVT constant conditions. We set a_0, the lattice constant, to 5.47 Å. As mentioned in the introduction, a TAD simulation derives the dynamics at low temperature T_l from the molecular dynamics simulation at high temperature T_h. In the following results, we show the dynamics at $T_l = 500$ K, estimated from the simulation at $T_h = 1500$ K for the migration of vacancies, and $T_h = 2000$ K for the migration of interstitial and interstitial cluster.

In the next section, we present the results of our simulations in detail. To describe the configuration and dynamics of atoms clearly, it is convenient to introduce coordinates in the system. We assume that U atoms on regular lattice sites are at (000), (100), (1/2 1/2 0), and so on. O atoms are then at (1/4 + l/2, 1/4 + m/2, 1/4 + n/2), where l, m and n are integers.

3. Simulation results

3.1. The migration of a single vacancy

First, we carried out a simulation when one O vacancy is introduced. We show the typical migration process in Fig. 1. In the left figure, the vacancy exists in the bottom-right corner of the figure. After a short-time, the O atom to the left of the vacancy moves to the vacant lattice site, which results in the motion of the vacancy to the left. After the transition, shown in the right figure, the vacancy is at the bottom-middle of the figure. Here, we note that the interval of the transition is very short, $\sim 3.5\times10^{-10}$ s. We performed a long-time simulation of vacancy migration, and found that the interval of hopping is about 10^{-10}–10^{-11} s. This quick migration can be explained by the small transition state energy. We calculate the transition state energy ΔE, defined by the difference between the energy of the saddle state and that of initial state, using the nudged elastic band (NEB) method [18]. We find $\Delta E = 0.26$ eV, which is consistent with that found by Govers et al. $\Delta E = 0.3$ eV [19].

3.2. The migration of a single interstitial

Though the migration of an O vacancy is simple, that of oxygen interstitial is a somewhat more complex. In Fig. 2, we show a typical example of the migration of a single oxygen interstitial. Before migration, the interstitial is at (1/2 1/2 1/2). The migration process is described as follows. First, the interstitial oxygen atom moves in a $\langle\bar{1}\,\bar{1}\,\bar{1}\rangle$ direction, and pushes out the oxygen atom at (1/4 1/4 1/4), as shown in the middle figure. The pushed out oxygen atom then moves to (−1/2 −1/2 1/2) and becomes a new interstitial.

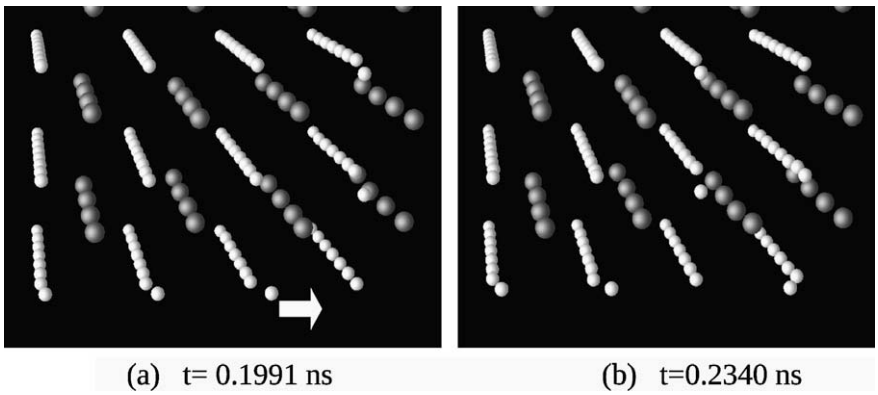

Fig. 1. Snapshot of the migration process of an oxygen vacancy: (a) at $t = 0.1991$ ns and (b) at $t = 0.2340$ ns. Gray balls and white balls represent uranium atoms and oxygen atoms, respectively. White arrow indicate the direction of motion of oxygen atom.

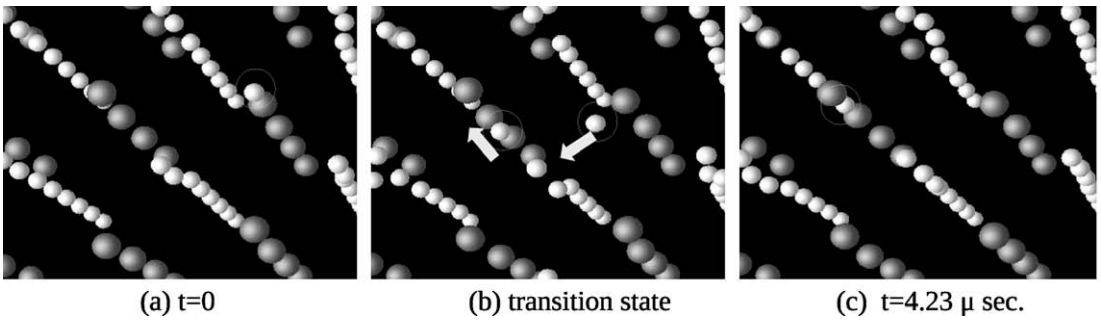

Fig. 2. Snapshot of the migration process of a single oxygen interstitial: (a) at $t = 0$, (b) the transition state and (c) at $t = 4.23$ μs. These figures show that the movement of interstitial oxygen involves the movement of two oxygen atoms, marked by circles. The arrows in the middle figure indicate the direction of motion of the two oxygen atoms.

We note that the migration of the single interstitial is much slower than that of the vacancy. Our simulation shows that the hopping occurs about 10^5—10^6 times in a second. This value is 10^5—10^6 times smaller than that of the vacancy, which is on the order of 10^{11}. We can explain this large difference qualitatively by the difference in the transition state energy. Using the NEB method, we obtain a transition state energy $\Delta E = 0.94$ eV. This is much larger than that for vacancy migration, and enough to explain the difference in the hopping rates. We also note that this transition state energy is much smaller than that obtained by Govers et al.. They found $\Delta E = 1.3$ eV for the migration of the oxygen interstitial with Basak potential. This inconsistency is due to the method for finding the transition state energy. The energy of the stable state can be easily obtained by using well-known algorithms like the conjugate gradient method. On the other hand, it is much more difficult to calculate the transition state energy. Govers et al. used rational-function optimization [20] for the calculation, while we employed the NEB method. The migration process obtained by these two methods are similar, however, the energy they obtained is much larger than ours.

3.3. The migration of clusters containing vacancies

It is well-known that defect clusters often exhibit quick migration [21,22]. To investigate the possibility of such processes in UO_2, we study the dynamics of defect clusters in UO_2. In this section, we briefly describe the results for vacancy clusters.

First, we performed a simulation of clusters made from two oxygen vacancies. As an initial condition, we put the two vacancies at (1/41/41/4) and (3/41/41/4). However, such a cluster is unstable. Due to the repulsive Coulomb interaction between oxygen vacancies, the cluster breaks apart completely within 10^{-10} s. The barrier for the break-up of vacancy clusters is about 0.13 eV. This result suggests that the vacancy cluster is unstable at 500 K.

We also simulated the situation when one O interstitial and one O vacancy coexist as an oxygen Frenkel pair. However, we find that such a pair recombined quickly even when the initial distance between defects is large. For example, we performed a simulation when the vacancy and the interstitial are initially at (1/4,1/4,1/4) and (0,1/2,2). The distance between these two defects is 9.77 Å, which is about a half of the system size of the simulation. Due to the long range Coulomb force, the vacancy is strongly attracted to the interstitial, and recombination occurs within 10^{-10} s.

3.4. The migration of the two interstitial cluster

Now, we present results for clusters made from two O interstitial atoms. In contrast to the case mentioned above, two interstitials make a stable cluster. The structure of the cluster is described in Fig. 3. The main part of the structure is constructed from three interstitials at (1/200), (01/20), (1/200) and one vacancy at (1/41/41/4). As Govers et al. discuss, such a structure is the energy minimum for many potentials. Here we should also pay attention to the displacement of oxygen atoms close to this cluster. The oxygen atoms at (3/41/41/4) and (1/41/43/4) are strongly displaced, and these atoms move close to (3/41/41/2) and (1/21/43/4), respectively. Interestingly, the displacement of the oxygen atom at (1/43/41/4) is small. This result indicates that this cluster has very low symmetry.

We find that this cluster migrates very quickly in the UO_2 crystal. To understand the diffusion mechanism of this cluster, we investigate the transition state of the migration process. We find that there are three kinds of movement, depicted in Fig. 4, that

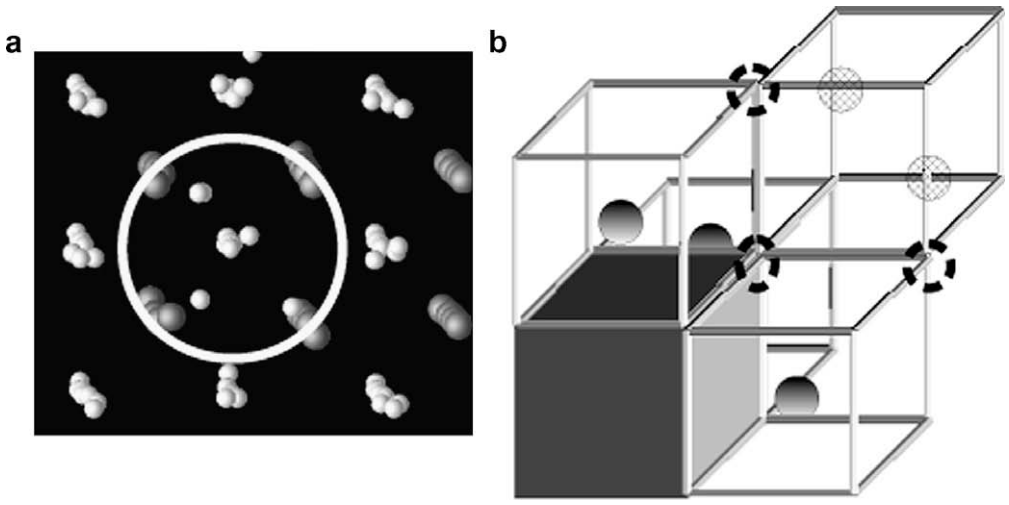

Fig. 3. (a) Stable structure of clusters made from two interstitial oxygens and (b) its schematic figure. The cube represents the lattice made from oxygen atoms. The gray cube indicates that an U atom exists at the center of the cube. Filled, hatched, and empty circles represents the interstitials, displaced oxygen atoms and vacancies, respectively. These figures show that the cluster is made from three interstitials, one vacancy, and two displaced oxygen atoms.

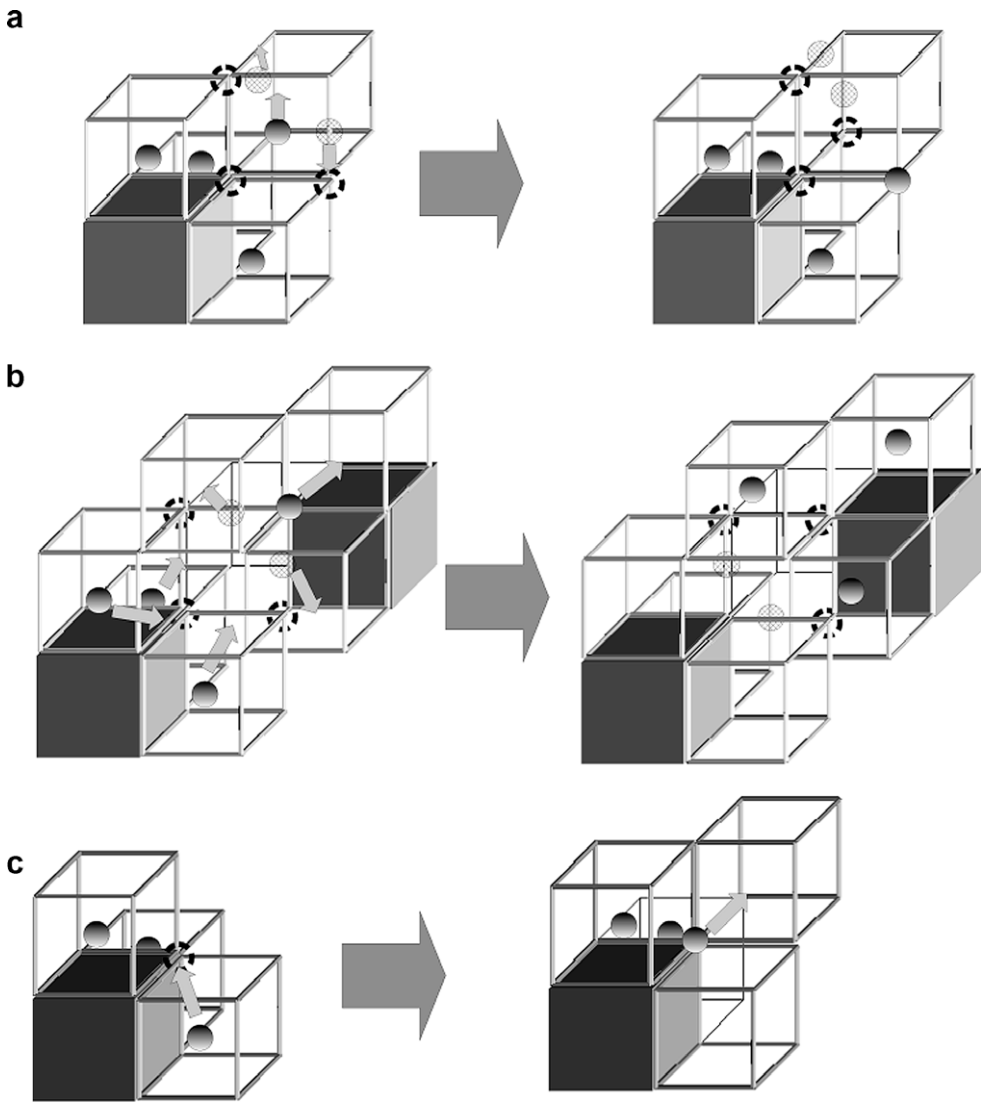

Fig. 4. Three movement of interstitial clusters. The transition state energy in each process is (a) 0.14 eV, (b) 0.16 eV and (c) 0.19 0.24 eV. Arrows in this picture show the direction of movement of each oxygen atoms.

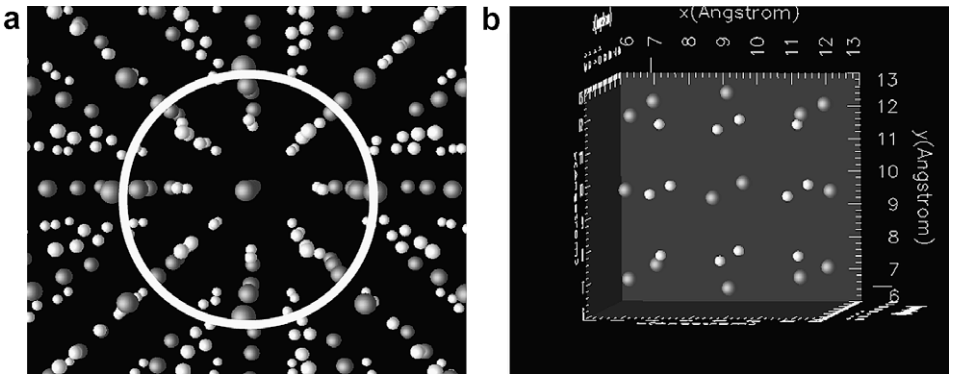

Fig. 5. (a) The stable configuration of atoms which includes four oxygen interstitials. The interstitial cluster is surrounded by circle. (b) The structure of the interstitial cluster. The oxygen atoms, depicted by white circle, forms cuboctahedral structure.

have small transition energies. Now we explain these processes in detail.

The process that has the lowest transition state energy is described at Fig. 4(a). In this process, the change in the position of the three interstitials at (1/200), (01/20) and (001/2) is small. On the other hand, the atoms at (3/41/41/2), (1/21/43/4) and (1/43/41/4) move to (3/41/41/4), (1/41/23/4) and (1/43/41/2), respectively. The configuration of atoms after the transition is essentially the same as the initial state, as we can obtain this configuration by rotating the initial state $2\pi/3$ around the $\langle 111 \rangle$ axis. The transition energy of this process is 0.14 eV.

The second process, which has a transition state energy of 0.16 eV, is depicted in Fig. 4(b). In this process, the six oxygen atoms at (1/200), (01/20), (001/2), (3/41/41/2), (1/21/43/4) and (3/41/43/4) change their position. The three interstitial atoms at (1/200), (01/20), (001/2), move to (1/21/41/4), (1/41/21/4), (1/41/41/4) respectively, and these atoms are not interstitials after the transition. On the other hand, the atoms at (3/41/41/2), (1/21/43/4) and (3/41/43/4) in the initial state become interstitials at (101/2), (1/201) and (11/21). These interstitials surround the vacancy at (3/41/43/4).

Though these two processes may enhance the migration of clusters, another process is needed for net migration. We can realize this by noticing that the vacancy is always at the nearest neighbor position of (1/21/21/2). In the first process, the vacancy does not move at all. In the second process, the vacancy moves from (1/41/41/4) to (3/41/43/4), however, it is still nearest neighbour of (1/21/21/2). By combination of these two processes, the vacancy can move to other positions such as (1/43/43/4) or (3/43/41/4). However, it is always at the nearest neighbour position of (1/21/21/2). Therefore another process is necessary for the true migration of this cluster.

The third process, which is essential for migration, is simpler than the other two. We depict this process in Fig. 4(c). In this process, one of the three interstitials combines with the vacancy and a di-interstitial state appears as a saddle. For example, the interstitial at (1/200) moves to (1/41/41/4). However, this state is unstable, and one of the O atoms neighboring the two remaining interstitials, either at (1/41/41/4) or at (−1/41/41/4), moves. The transition state energy of this process is 0.19–0.24 eV. The small variation in the transition energy reflects the fact that the three interstitials are not equivalent, due to the asymmetric displacement of O atoms in the lattice. This process leads to migration of the cluster, in contrast to the two processes we have mentioned above.

Via these three mechanisms, this cluster migrates very quickly. As is evident from the transition state energy, the interval of transition is about 10^{-11}–10^{-12} s, which is the same as or a little shorter than that of vacancies. Such fast migration of clusters has been reported in many materials such as MgO [22].

We have found that there are additional migration processes, however, their transition state energies are larger than 0.4 eV. Therefore the dominant migration mechanisms are the three processes we described above.

3.5. Complex structures formed from three or more interstitials

We have shown that clusters made of two interstitials demonstrate fast migration. It is then natural to ask what happens when more interstitials are clustered. To answer this question, we carried out simulations for the cases where three and four interstitials are included. As the initial condition, we put three and four oxygen interstitials in clusters. In the case of three interstitials, we find that there are some local energy minima, and the transition state energies between these minima are small, $\Delta E \lesssim 0.1$ eV. The acceleration mechanism of the TAD method does not work for the simulation conditions, and we can only investigate the dynamics over a short period. However, the clusters do not dissociate in the time scale $\sim 10^{-9}$ s.

In the case of four interstitials, we find a stable configuration, which shows no diffusion. The stable structure is depicted in Fig. 5. This configuration have a cuboctahedral arrangement of interstitial oxygen atoms, which is similar to the one proposed for the crystal structure of U_4O_9 [23]. Though it seems that the system has a cubic symmetry, the oxygen atoms around the cuboctahedral clusters are strongly distorted, and the symmetry is broken. This lost of symmetry implies that there are some equivalent configurations of atoms which have the same energy. The transition process which has the lowest saddle point energy is the transition between these equivalent configurations. The transition state energy of this process is 1.765 eV. The processes which cause the migration or break of this cluster have higher transition energy, and we conclude that the cluster is immobile and stable.

4. Summary of computational results and discussion

We performed TAD simulations to investigate the dynamics of anion point defects in UO_2. In the case of single defects, the diffusion of the vacancy is much faster than that of the interstitial. However, clusters made from two interstitials diffuse as fast as vacancies. In our case, the stable structure is one vacancy surrounded by three interstitials. This cluster migrates through a saddle structure which includes two interstitials.

There are many experiments which suggest the fast migration of excess oxygen in UO_2 [24,25]. However, it is difficult to simulate

such fast migration. To carry out a MD simulation of migration in a reasonable time, we must raise the temperature. Moreover, the transition state energy of interstitials is much higher than that of vacancies for most potentials, which indicates the slow diffusion. Our result shows that interstitial clusters can diffuse faster than the vacancy, while single interstitials show slow migration. Though our results are obtained by the simulation in small system with a specific potential, we suppose that the fast migration of interstitial clusters also occurs through a similar mechanism in large systems with other potentials. Concerning with the smallness of system, it is a difficult task to carry out the TAD simulation in larger systems. However, if the two stable configurations of atoms are given, it is not difficult to obtain the transition state energy between them. We made the calculation of the stable configuration of atoms and transition state energy in $6 \times 6 \times 6$ superlattice. We find that the structure composed of three interstitials and one vacancy is stable, while that of two interstitials is unstable. We also find the transition state energy 0.21 eV, which is consistent with the results of the TAD simulation in $4 \times 4 \times 4$ superlattice. Therefore we believe that the our results is also valid for larger system.

Concerning with the potential, the structure composed of three interstitials and one vacancy gives a minimum energy state for most UO_2 potentials [19]. The third process in the previous section seems a natural process for the diffusion of such a cluster. Moreover, it is found that the Grimes potential and density-functional theory gives a similar, slightly different, mechanism for cluster diffusion [26]. In the case of the Grimes potential, both the two interstitial state and the three interstitial + one vacancy state are stable, and there is a saddle between these two states. In our results, the two interstitial state is a saddle, not a stable state. We will need further investigation to clarify the diffusion mechanism of interstitials in UO_2. However, these results suggest the importance of the change between the two configurations for the migration of clusters.

As mentioned previously, it is well known that clustered defects in metals show much faster migration than single point defects [21]. Our result shows that such phenomena can occur also in ceramic materials. We note that there exists some differences between the migration of clusters in these two materials. First, the rate of migration strongly depends on the size of clusters. Though the two interstitial cluster shows rapid migration, the four interstitial cluster is non-diffusive. On the other hand, the rate of migration increases as the size of the cluster increases in metals. Second, the diffusion in metals is one-dimensional with clusters moving in one direction. In the case of UO_2, the direction of the motion is not one-dimensional. Therefore there is a great difference between the diffusion of defects in metals and in ceramics. However, our result implies the importance of defect clusters for understanding the dynamics of dislocations in ceramic materials.

Our result also gives some constraints on kinetic models of self-organization in UO_2. It is hard to carry out atomic simulations for large systems, and a more macroscopic model is needed to complement the weaknesses of microscopic simulations. One candidate of such an approach is a kinetic model based on rate equations. For example, void-lattice formation in irradiated metals can be explained successfully with this method [27]. In this approach, the density of dislocations and point defects are treated by reaction-diffusion equations. Our simulations suggest the dynamics of defect clusters strongly depends on their size. The diffusion of single interstitials is much slower than that of di-interstitial clusters, while four interstitial clusters are immobile. This result implies that the density of interstitials, di-interstitial clusters, and four interstititial clusters should be included for reaction-diffusion equations. The difference of diffusion rates between different elements often leads to pattern formation through the Turing instability.

Our results shed light on formation mechanism of the rim structure in UO_2. As we have mentioned in the introduction, the emergence of the planar defects is intimately connected to the formation of the rim structure. Therefore the understanding of the process of planar defect formation will give us important insight into the mechanism of the rim structure formation. In this paper, we studied the migration processes of interstitials, and found that interstitial clusters plays a dominant role. By studying the interactions of these clusters, we expect to clarify the detail of the planar defect formation, which is one of the key process of high-burnup fuel performance of LWR fuels.

5. Summary

We have studied the migration process of oxygen defects in UO_2 using temperature accelerated dynamics method with two-body interatomic potential of Basak. Though the migration of single oxygen interstitial is very slow, we find that the cluster of the interstitials shows very quick migration. We also find that the four interstitials forms a stable, immobile clusters. These findings suggest the importance of clustering of defects in the formation of high-burnup structure.

Acknowledgements

We acknowledge A.F. Voter for his help in the development of the simulation code. We would also like to acknowledge Los Alamos National Laboratory for supporting the collaboration, providing working infra-structure including communication and computational environment.

This work is financially supported by the Budget for Nuclear Research of the Ministry of Education, Culture, Sports, Science and Technology of Japan, based on the screening and counseling by the Atomic Energy Commission. Work at LANL was funded by the Office of Science, Office of Basic Energy Sciences. Los Alamos National Laboratory is operated by Los Alamos National Security, LLC, for the National Nuclear Security Administration of the US DOE under contract DE-AC52-06NA25396.

References

[1] M.L. Bleiberg, R.M. Berman, B. Lustman, in: Proceedings of Symposuim on Radiation Damage in Solids and Reactor Materials, IAEA, Vienna, 1963. p. 319.
[2] D. Baron, in: Nineth HBEP Review (1986).
[3] M. Kinoshita, T. Sonoda, S. Kitajima, A. Sasahara, E. Kolstad, Hj. Matzke, V.V. Rondinella, A.D. Stalios, C.T. Walker, I.L.F. Ray, M. Sheindlin, D. Halton, C. Ronch, in: Proceedings of International Conference on LWR Fuel Performance, 2000, p. 590.
[4] M. Kinoshita, H.Y. Geng, Y. Chen, Y. Kaneta, M. Iwasawa, T. Ohnuma, T. Sonoda, L. Yasunaga, S. Matsumura, K. Yasuda, M. Sataka, N. Ishikawa, Y. Chimi, J. Nakamura, M. Amaya, in: Proceeding of Top Fuel 2006, International Meeting on LWR Fuel Performance, 2006, p. 132.
[5] L.E. Thomas, C.E. Beyer, L.A. Charlot, J. Nucl. Mater. 188 (1992) 80.
[6] I.L.F. Ray, H. Thiele, Hj. Matzke, J. Nucl. Mater. 188 (1992) 90.
[7] L.F. Ray, Hj. Matzke, H.A. Thiele, M. Kinoshita, J. Nucl. Mater. 245 (1997) 115.
[8] K. Yasunaga, K. Yasuda, S. Matsumura, T. Sonoda, Nucl. Inst. Meth. B 250 (2006) 114.
[9] T. Sonoda, M. Kinoshita, Y. Chimi, N. Ishikawa, M. Sataka, A. Iwase, Nucl. Inst. Meth. B 250 (2006) 254.
[10] E.M. Bringa, R.E. Johnson, Phys. Rev. Lett. 88 (2002) 165501.
[11] M. Toulemonde, Ch. Dufour, A. Meftah, E. Paumier, Nucl. Inst. Meth. B 166&167 (2000) 903.
[12] Hj. Matzke, Radiat. Eff. Def. Solids 75 (1983) 317.
[13] M. Iwasawa, Y. Chen, Y. Kaneta, T. Ohnuma, Mater. Trans. 47 (2006) 2651.
[14] H.Y. Geng, Y. Chen, Y. Kaneta, M. Kinoshita, Phys. Rev. B 75 (2007) 54111.
[15] M.R. Sørensen, A.F. Voter, J. Chem. Phys. 112 (2000) 9599.
[16] C.B. Basak, A.K. Sengpta, H.S. Kamath, J. Alloys Compd. 360 (2003) 10.
[17] H.Y. Geng, Y. Chen, Y. Kaneta, M. Kinoshita, J. Alloys Comp. 457 (2008) 465.
[18] H. Jónsson, G. Millis, K.W. Jacobsen, in: B.J. Berne, G. Ciccotti, D.F. Coker (Eds.), Classical and Quantum Dynamics in Condensed Phase Simulations, World Scientific, 1998.
[19] K. Govers, S. Lemehov, M. Hou, M. Verwerft, J. Nucl. Mater. 366 (2007) 161.
[20] A. Banerjee, N. Adams, J. Simons, R. Shepard, J. Phys. Chem. 89 (1985) 52.

[21] S. Ishino, N. Sekimura, H. Abe, J. ASTM Int. 4 (2007). paper ID: JAI100644.
[22] B.P. Uberuaga, R. Smith, A.R. Cleave, F. Montalenti, G. Henkelman, R.W. Grimes, A.F. Voter, K.E. Sickafus, Phys. Rev. Lett. 92 (2004) 115505.
[23] D.J.M. Bevan, I.E. Grey, B.T.M. Willis, J. Solid State Chem. 61 (1986) 1; L. Nowicki, F. Garrido, A. Turos, L. Thomé, J. Phys. Chem. Solids 61 (2000) 1789; H.Y. Geng, Y. Chen, Y. Kaneta, M. Kinoshita, Phys. Rev. B 77 (2008) 180101.
[24] H. Assmann, W. Dorr, M. Peehs, J. Nucl. Mater. 140 (1986) 1.
[25] T. Ishii, K. Naito, K. Oshima, J. Nucl. Mater. 36 (1970) 288.
[26] D.A. Andersson, C. Deo, B.P. Uberuaga, (in preparation).
[27] K. Krishan, Nature 287 (1980) 420.